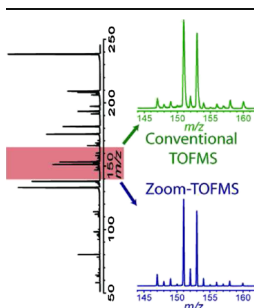


## RESEARCH ARTICLE

# Inductively Coupled Plasma Zoom–Time-of-Flight Mass Spectrometry

Elise A. Dennis,<sup>1</sup> Steven J. Ray,<sup>1</sup> Christie G. Enke,<sup>2</sup> Gary M. Hieftje<sup>1</sup><sup>1</sup>Department of Chemistry, Indiana University, Bloomington, IN 47405, USA<sup>2</sup>Department of Chemistry and Chemical Biology, University of New Mexico, Albuquerque, NM 87131, USA

**Abstract.** A zoom–time-of-flight mass spectrometer has been coupled to an inductively coupled plasma (ICP) ionization source. Zoom–time-of-flight mass spectrometry (zoom-TOFMS) combines two complementary types of velocity-based mass separation. Specifically, zoom-TOFMS alternates between conventional, constant-energy acceleration (CEA) TOFMS and energy-focused, constant-momentum acceleration (CMA) (zoom) TOFMS. The CMA mode provides a mass-resolution enhancement of 1.5–1.7 $\times$  over CEA-TOFMS in the current, 35-cm ICP-zoom-TOFMS instrument geometry. The maximum resolving power (full-width at half-maximum) for the ICP-zoom-TOFMS instrument is 1200 for CEA-TOFMS and 1900 for CMA-TOFMS. The CMA mode yields detection limits of between 0.02 and 0.8 ppt, depending upon

the repetition rate and integration time—compared with single ppt detection limits for CEA-TOFMS. Isotope-ratio precision is shot-noise limited at approximately 0.2% relative-standard deviation (RSD) for both CEA- and CMA-TOFMS at a 10 kHz repetition rate and an integration time of 3–5 min. When the repetition rate is increased to 43.5 kHz for CMA, the shot-noise limited, zoom-mode isotope-ratio precision is improved to 0.09% RSD for the same integration time.

**Keywords:** Inductively coupled plasma, Zoom-TOF, Time-of-Flight, Mass spectrometry

Received: 26 August 2015/Revised: 9 November 2015/Accepted: 12 November 2015/Published Online: 3 December 2015

## Introduction

The inductively coupled plasma (ICP) has become the most widely used ion source for elemental mass spectrometry and has found application in fields as diverse as geology and pharmaceuticals [1]. When coupled with mass spectrometry, the ICP offers low (sub-ppt) detection limits, broad dynamic range, and both qualitative and quantitative analysis of ultra-low sample volumes [1, 2]; it has been used to determine metal content in single cells [3]. For instance, the emerging field of mass cytometry utilizes the high sensitivity of ICP-MS to determine cellular makeup by use of isotopically distinct metal tags [3–5]. The analytical performance of an ICP-MS system is, however, strongly dependent on the type of mass analyzer employed [6].

Recent advances in TOFMS have focused on enhancing mass resolution. In the last 15 years, multi-turn and multi-pass instruments have reported mass resolution in the high tens-of-thousands, approaching the lower end of resolution for Fourier-transform systems [7–12]. Yet, single-reflectron TOFMS instruments are the most common because they are useful for the study of transient events such as are produced by laser ablation [13–16], chromatography [17–19], and electrothermal (furnace) vaporization [20, 21]. Zoom-TOFMS is an alternative approach for mass-resolution enhancement in existing or purpose-made single-reflectron TOFMS systems and provides an even higher duty factor than conventional single-reflectron TOFMS [22].

The zoom-TOFMS concept is simple—two complementary types of TOFMS [conventional, constant-energy acceleration (CEA) and energy-focusing, constant-momentum acceleration (CMA)] are utilized in separate operating modes on a single instrument [22]. The CEA-TOFMS mode delivers all the benefits of conventional TOFMS, including a theoretically unlimited (but practically limited) mass range, excellent detection limits, and a dynamic range of  $10^4$ – $10^5$  [12, 23]. The CMA-TOFMS (zoom) mode is an attractive complement to CEA-

**Electronic supplementary material** The online version of this article (doi:10.1007/s13361-015-1309-5) contains supplementary material, which is available to authorized users.

Correspondence to: Gary M. Hieftje; e-mail: hieftje@indiana.edu

TOFMS because CMA-TOFMS can enhance mass resolution by 1.5 to 1.7 times and improve speed, duty factor, and therefore sensitivity, albeit over a limited, selectable mass range [22].

The CEA- and CMA-TOFMS operational modes make use of different focusing mechanisms. In particular, the conventional, CEA-TOFMS mode makes use of space-focusing principles whereas the zoom CMA-TOFMS mode focuses ions based on their energies. The concept of space-focusing in CEA-TOFMS is well established as is the use of a reflectron to mirror the space focus and to partially compensate for ion-energy disparities [23]. The concept of energy-focused CMA was introduced in 2007 [24] and has been applied to both distance-of-flight MS (DOFMS) [25–31] and TOFMS [22, 32, 33].

The CMA mode of zoom-TOFMS enhances resolution at a specific energy-focus time ( $t_{ef}$ ). At  $t_{ef}$ , all ions, regardless of their  $m/z$ , are energetically focused at  $m/z$ -dependent locations along the mass-separation axis [24]. The specifics of the energy focus achieved at  $t_{ef}$  are detailed elsewhere [24, 32, 33]. At  $t_{ef}$ , initial ion velocities are focused while initial spatial distributions are maintained, which means that ion turnaround times in the acceleration region do not compromise resolution. Also, in CMA mode  $m/z$  and flight time are directly related (as opposed to quadratically related in CEA-TOFMS). Therefore, for those ions detected at (or near)  $t_{ef}$ , mass resolution is improved over CEA-TOFMS operation [22]. Moreover, since any desired narrow mass range can be selected with CMA-TOFMS, it is also possible to improve instrument sensitivity through mass-range isolation and use of a higher repetition rate (demonstrated up to 100 kHz) [22].

In the current study, analytical performance of an ICP-zoom-TOFMS instrument is evaluated. Enhanced mass resolution in CMA zoom mode is verified with a multi-element standard solution and achievable resolution for both CEA and CMA operating modes is determined for several atomic mass windows. Isotope-ratio precision in both operating modes is also evaluated and compared with that of other state-of-the-art ICP-MS technologies. Sensitivities, detection limits, and dynamic range are also evaluated for both operating modes of zoom-TOFMS.

## Experimental

The zoom-TOFMS instrument was previously used for distance-of-flight mass spectrometry (DOFMS) [26–31, 33, 34] and is described here for the first time as a TOFMS system. Very few instrument modifications were required for conversion to zoom-TOFMS. Specifically, a microchannel plate (MCP) detection system and a retarding potential analyzer (RPA, also known as energy-discrimination system) were added to the existing instrument platform. A schematic of the ICP-zoom-TOFMS instrument is shown in Figure 1.

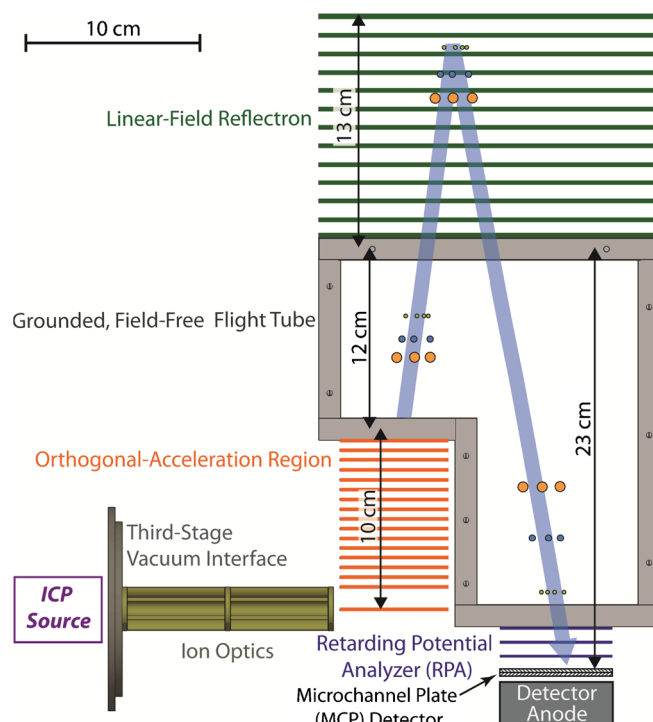


**Figure 1.** Schematic of the orthogonal-acceleration and mass-separation regions of the ICP-zoom-TOFMS instrument

### Sample Preparation, Introduction, and Ionization

The 40.68 MHz ICP ionization source (crystal-controlled, model HF 2000F; PlasmaTherm Inc., Kresson, NJ, USA) used in this study has been previously described in detail [29, 30]. Commercially available analytical reagent grade 1000 ppm stock solutions or analytical reagent grade nitrate salts (from several different manufacturers) were used to prepare all sample and standard solutions. Specific-resistance deionized water (18.2 M $\Omega$ ) with HNO<sub>3</sub> from an in-house, sub-boiling polytetrafluoroethylene distillation unit was used to prepare 0.1 M HNO<sub>3</sub> for dissolution (or dilution) of salts and standards. For all experiments, samples were introduced into the ICP by means of a 0.6–0.8 L/min argon flow (>99% purity; Airgas, Inc., Radner, PA, USA) from an ultrasonic nebulizer with a membrane desolvator unit (Cetac U-6000 AT+; Cetac Technologies, Omaha, NE, USA). Sample solutions were introduced into the ultrasonic nebulizer at 1 mL/min by a peristaltic pump (Minipuls 2; Gilson Inc., Middleton, WI, USA). Once nebulized, the sample solutions entered the ICP as an aerosol, where they were atomized and ionized, and the resulting species entered the three-stage differentially pumped vacuum interface. The vacuum interface has been described elsewhere [26, 29]. The pressures were approximately 0.7 Torr, 0.5 mTorr, and 0.7  $\mu$ Torr in each of the three vacuum stages, respectively. A recirculating chiller (Neslab model CFT-75; Thermo Scientific, Ashville, NC, USA) was used to cool the first and second vacuum stages to 10°C.

### *Ion Optics and Mass Analyzer*

After passing through the vacuum interface, the ion beam is shaped by a set of DC quadrupole doublet ion optics followed by a slit optic [26]. The slit optic narrowly confines the ion beam as it passes into the orthogonal-acceleration region. There, ions are accelerated either to a constant energy or a constant momentum, depending upon the desired operational mode. A square-shaped, high-voltage (1 kV) pulse with a rise/fall time of less than 25 ns was generated by a high-voltage pulser (DEI PVX-4150; Directed Energy, Inc., Boulder, CO) and a high-voltage power supply (210-01R, Bertan Associates, Inc., Hicksville, NY, USA) for ion acceleration. To achieve constant-energy acceleration (CEA), ions experience the orthogonal-acceleration pulse over the entire 10-cm acceleration region. In the case of CMA, the acceleration pulse is terminated before ions within the target mass range exits the acceleration region.

The repetition rate of the orthogonal-acceleration pulse in both operational modes was set to 10 kHz unless otherwise specified. Since only a narrow target mass region is detected with CMA-TOFMS, and ions have  $m/z$ -dependent energies, it is possible simply to mass-select that target region [22]. Mass-range selection was performed in this study by means of ion-energy filtering. Specifically, the reflectron and the RPA were used here to filter out  $m/z$  values below and above the target mass region, respectively. Once the target mass window was selected, the repetition rate was increased to 43.5 kHz to improve instrumental duty factor. Ion-energy filtering for energy-focused CMA-TOFMS has been described previously [22].

Once accelerated, ions enter a 12-cm long field-free mass-separation region, are turned around in a 13-cm deep linear-field reflectron, and travel through a second, 23-cm long field-free region (cf. Figure 1). At 35 cm along the flight path a RPA was installed. The RPA setup consists of three stainless-steel electrodes with nickel-mesh grids oriented parallel to each other and perpendicular to the mass-separation axis, and separated by 0.25-cm ceramic spacers. The RPA was used to create a potential barrier along the flight path to filter out low energy ions before detection. A similar RPA system has been used in CMA-TOFMS to efficiently remove ions with  $m/z$ -values greater than the target mass region [22]. After the RPA, ions travel an additional 0.64 cm before striking the matched pair of 40-mm extended-dynamic-range microchannel plates (MCPs) (Photonis USA, Inc., Sturbridge, MA, USA). The total field-free mass-separation region length in the ICP-zoom-TOFMS instrument is 35 cm.

### *Mass Spectral Acquisition*

Ion signal from the MCPs was recorded either by ion counting or analog ion-current averaging. For ion counting, an Ortec 9308 picosecond time analyzer (Oak Ridge, TN, USA) with a Tennelec TC454 four-channel constant-fraction discriminator (Oak Ridge, TN, USA) was employed to record ion arrival times. The Ortec 9308 has a 50 ns dead time after each

detection event, during which no additional ions can be detected. A non-inverting fast preamplifier (VT120A; Ortec, Inc.) was used to amplify the output current from the MCPs in analog detection mode before the signal was recorded and digitized by a 2.5-GHz digital phosphor oscilloscope (TDS 7254; Tektronix, Inc., Richardson, TX, USA). Ion counting was employed for mass-spectral acquisition when the sample concentration was  $\leq 10$  ppb and analog detection was used for concentrations above 10 ppb. Mass spectra were analyzed by a combination of LabVIEW® 2010 (National Instruments, Austin, TX, USA), OriginPro (2015 version; OriginLab Corp, Northampton, MA, USA), and Microsoft Excel 2010.

## Results and Discussion

Sample analysis with zoom-TOFMS is straightforward and consists of a full-spectrum acquisition in CEA (conventional) TOFMS mode followed by one or more targeted mass-spectral collections in CMA (zoom) TOFMS mode. The initial CEA-TOFMS analysis provides both qualitative and quantitative information about all sample constituents, whereas the subsequent CMA-TOFMS analyses provide more detailed, targeted spectral information [22]. In order to alternate between CEA- and CMA-TOFMS operations, several instrument parameters need adjustment. These parameters include the acceleration pulse, the reflectron voltage, and the ion-optic potentials. The acceleration pulse parameters (duration and potential) and the reflectron potential are adjusted to ensure proper space and/or energy focusing in each operational mode and for selecting the target mass range(s) during zoom operation [22, 32, 33]. The ion-optic potentials must be switched between CEA- and CMA-TOFMS because the optimal pre-acceleration ion-beam shape is different [32, 33]. These changes are currently performed manually, but could easily be automated.

A multi-element solution was analyzed by ICP-zoom-TOFMS to assess operation with a high peak-density mass spectrum. The multi-element solution contained 19 elements ranging from nickel ( $m/z$  58–64) to uranium ( $m/z = 234$ –238), all at 1 ppm concentration. Figure 2 shows the resultant mass spectra in both a single CEA-TOFMS spectrum (black trace at top) and in CMA-TOFMS mode as 11 stitched-together mass spectra (multicolored at bottom). The focus of this analysis was to produce the strongest ion signal at each  $m/z$  in both operating modes. Even so, the resulting resolving power (full-width at half-maximum,  $RP_{FWHM}$ ) for CMA-TOFMS peaks was on average 1.7 times better than for CEA-TOFMS peaks.

All peaks in the 11 CMA-TOFMS (zoom-mode) spectra exhibit higher mass resolution than those in the CEA-TOFMS spectrum. Of course, the optimal  $RP_{FWHM}$  is observed for  $m/z$  values detected at or near  $t_{ef}$ . The  $m/z$  range within this optimal focus window has been discussed in detail previously [32] and is between two and 18 mass units for singly charged atomic species. In practice, even the edges of the  $m/z$  target window in zoom mode offer better  $RP_{FWHM}$  than that seen with CEA-TOFMS. The



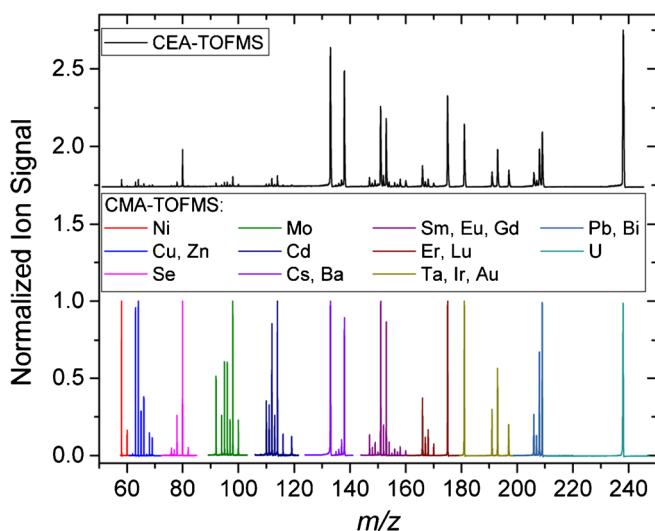


**Figure 2.** Demonstration of zoom-TOFMS for a multi-element standard solution containing 1 ppm of Ni, Cu, Zn, Se, Mo, Cd, Cs, Ba, Sm, Eu, Gd, Er, Lu, Ta, Ir, Au, Pb, Bi, and U. The trace shown in black at the top is an average of five individual CEA-TOFMS mass spectra. Ion signals have been normalized to the uranium peak at  $m/z$  238 and the baseline is offset by 1.75 for ease of comparison with CMA-TOFMS. The multicolored traces at the bottom represent individual CMA-TOFMS spectra taken for different energy-focus (selected mass-range) conditions. Each of the CMA-TOFMS spectra represents an average of five individual mass spectra and is normalized to the most intense mass-spectral feature

degradation of  $RP_{FWHM}$  away from  $t_{ef}$  is why 11 separate mass spectra are needed to cover the  $m/z$  58–238 range of the multi-element solution. Detection at a single  $t_{ef}$  also leads to peak heights that are distorted compared with those expected from natural isotopic abundances [32]; however, the relative peak *areas* represent the expected isotopic distributions.

Sensitivities for both the 11 CMA-TOFMS spectra and the single CEA-TOFMS spectrum in Figure 2 are compiled in Supplementary Table S-1. On average, the sensitivity [in counts per second per ppm (cps/ppm)] for the most abundant peak in each CMA-TOFMS spectrum was  $5.1 \times 10^7$  cps/ppm, and for the corresponding peak in the CEA-TOFMS spectrum the sensitivity was  $1.7 \times 10^6$  cps/ppm. The sensitivity difference between CEA- and CMA-TOFMS is likely a result of ion-focusing conditions. In CMA-TOFMS, the input ion beam need not be perfectly collimated (in fact, a focused beam is better [22]) for optimal operation, which means the focusing conditions are more forgiving to outliers. Also, it is probable that more ions pass through the slit optic into the acceleration region for the focused ion beam in CMA-TOFMS. Further, because of the nature of CMA-TOFMS, fewer argon ions are detected per acquisition as many are not turned around in the reflectron and are neutralized on the back plate of the flight tube. As a result, there is almost no detector recovery from argon detection in CMA-TOFMS, whereas detector recovery is pronounced in CEA-TOFMS.

### Zoom-TOFMS Mass Resolution

As Figure 2 shows, operation in zoom mode leads to improved mass resolution even in a routine scan optimized for maximum signal. However, even better resolution is possible if the instrument is optimized for that purpose. The maximum  $RP_{FWHM}$  for both the conventional CEA-TOFMS mode and the zoom CMA-TOFMS mode were evaluated for each of four atomic mass ranges, represented by isotopes of zirconium, europium, gadolinium, and lead (cf. Table 1). Lead yielded the largest  $RP_{FWHM}$  enhancement between modes (1.7 $\times$ ); the mass spectra for Pb by CEA- and CMA-TOFMS are shown in Figure 3.

The results in Table 1 and Figure 3 are consistent with a previous study on a 43-cm zoom-TOFMS instrument outfitted with a reduced-pressure, direct-current glow-discharge ion source [22]. The improvement in  $RP_{FWHM}$  reported for the 43-cm system was  $\leq 1.6$  times between CEA- and CMA-TOFMS and the maximum  $RP_{FWHM}$  was 1610 and 2550, respectively [22]. If we assume that  $RP_{FWHM}$  scales linearly with flight distance, the predicted maximum  $RP_{FWHM}$  for the current 35-cm ICP-zoom-TOFMS instrument would be 1300 for CEA-TOFMS and 2000 for CMA-TOFMS. Not surprisingly, the experimental values in Table 1 of 1100–1200 for CEA-TOFMS and 1700–1900 for CMA-TOFMS are slightly lower than these predictions. The ICP is a considerably hotter source than the glow discharge and produces ions with a wider range of energies [1, 35] and, consequently, somewhat broader mass-spectral peaks. For this reason, resolution would likely be improved with the use of a molecular (non-plasma) ionization source that produces a cooler ion beam for zoom-TOFMS. However, the 1.5–1.7 $\times$   $RP_{FWHM}$  improvement between operating modes is likely to remain regardless of the ion beam characteristics. Future investigations will evaluate zoom-TOFMS with molecular ionization sources.

Commercial single-reflectron ICP-TOFMS systems routinely produce mass resolution on the order of 1000–2500 for up to 1-m flight paths [36, 37]. The current 35-cm geometry ICP-zoom-TOFMS system performs well within that resolution range for both operational modes. If we extrapolate the average 1800  $RP_{FWHM}$  in Table 2 for zoom mode to 1 m of flight distance, the predicted  $RP_{FWHM}$  is approximately 5000. Unfortunately, a nominal resolving power of 7500 is needed to separate the notorious interference of  $ArCl^+$  from monoisotopic

**Table 1.** Highest  $RP_{FWHM}$  for Both the CEA- and CMA-TOFMS Operational Modes of Zoom-TOFMS for Four Mass Ranges Along with the Temporal Peak Width for Each Element. The Improvement in  $RP_{FWHM}$  Between CEA- and CMA-TOFMS is Also Reported

Element	CEA-TOFMS		CMA-TOFMS		$RP_{FWHM}$ improvement
	Peak width (ns)	$RP_{FWHM}$	Peak width (ns)	$RP_{FWHM}$	
Zr	10.6	1070	6.8	1710	1.6
Eu	11.8	1230	8.6	1720	1.4
Gd	12.3	1210	8.8	1720	1.4
Pb	14.8	1140	9.1	1930	1.7
Average	12.4	1160	8.3	1770	1.5

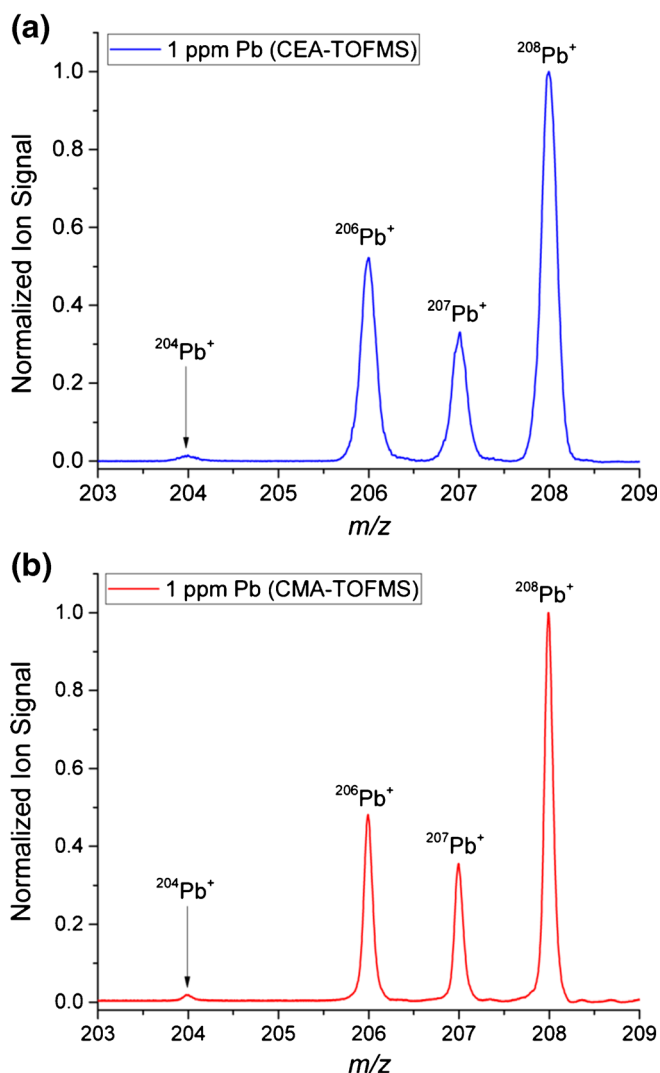


Figure 3. (a) CEA- and (b) CMA-TOFMS mass spectra for lead that correspond to the data in Table 1. The baseline fluctuations in both traces are due to an impedance mismatch in the detection system that causes ringing

As<sup>+</sup> when the concentrations are equivalent, but often a resolving power of 10,000 is needed due to much higher concentrations of ArCl<sup>+</sup>. However, it is likely that with further instrumental improvements, particularly to the ion optics and flight length, resolution for ICP-zoom-TOFMS would be able to conquer this and other spectral overlaps.

### Isotope-Ratio Precision

The ICP-zoom-TOFMS instrument was used to determine isotope-ratio precision with a 10 ppb europium solution. The % RSD of the <sup>151</sup>/<sup>153</sup> europium isotope ratio over a range of integration times is shown for both CEA- and CMA-TOFMS modes at a 10 kHz repetition rate (cf. Supplementary Figure S-1a and S-1b, respectively). The precision for the <sup>151</sup>Eu/<sup>153</sup>Eu ratio was also evaluated for CMA-TOFMS at a 43.5 kHz repetition rate (cf. Figure 4). In order to obtain a 43.5 kHz repetition rate, the reflectron and RPA were used as energy

**Table 2.** Single-Point Detection Limits ( $3\sigma$ ) for CEA- and CMA-TOFMS Operational Modes of Zoom-TOFMS. All Solution Concentrations were 100 ppt, 60-s Integration Times were used for Data Collection, and All LODs were Calculated Based on Peak Areas

Element	CEA-TOFMS LOD (ppt)		CMA-TOFMS LOD (ppt)		
	10 kHz	20 kHz	10 kHz	20 kHz	43.5 kHz
In	1.2	0.80	0.26	n/a	
Eu	3.2	0.21	0.11	0.084	
Gd	1.8	0.16	0.23	0.024	
Average	2.1	0.39	0.20	0.054	

filters to remove all ions outside the target mass window. With this higher repetition rate, two ion packets were undergoing mass separation at any given time.

All three plots for ICP-zoom-TOFMS precision (cf. Supplementary Figure S-1 and Figure 4) yield 0.08%–0.25% RSD for  $\leq 10$  min of integration time. The two-times lower (0.085%) RSD for the 43.5 kHz CMA-TOFMS experiment is expected compared to the 10 kHz case; at roughly four times the input pulse rate, the noise should be reduced by a factor of two. The slope of all three log-log plots (cf. Supplementary Figure S-1 and Figure 4) is approximately  $-0.5$ , indicating that the isotope-ratio precision is shot-noise limited. Overall, these results are consistent with previous studies of ICP-TOFMS instruments [38, 39] and with a DOFMS study on the same instrument platform with the same ICP source [29].

### Dynamic Range and Detection Limits

The dynamic range of the ICP-zoom-TOFMS instrument was evaluated in both operating modes. First, the linear dynamic range (LDR) for CEA-TOFMS was determined for samples of iridium. Supplementary Figure S-2 shows the LDR for <sup>191</sup>Ir<sup>+</sup> analyzed by CEA-TOFMS at a 10 kHz repetition rate to be at least six orders of magnitude. The calculated detection limit (by

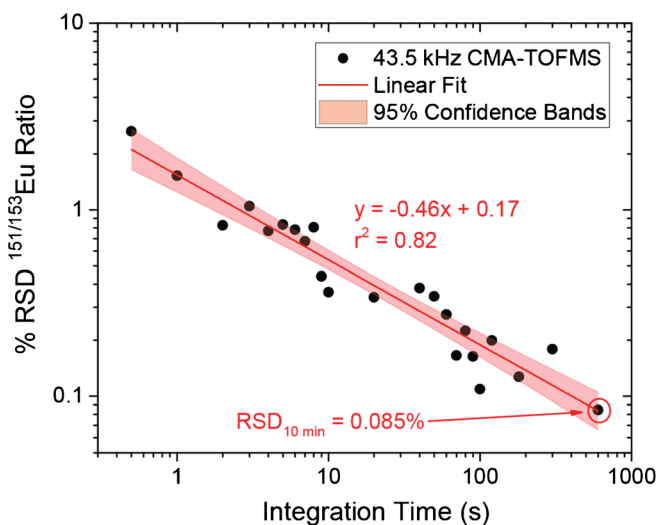


Figure 4. Effect of integration time on % RSD for the <sup>151</sup>/<sup>153</sup>Eu ratio with a 10-ppb europium solution analyzed with CMA-TOFMS at 43.5 kHz

the  $3\sigma$  definition) for  $^{191}\text{Ir}^+$  from Supplementary Figure S-2 is 3.4 ppt and the limit of quantitation ( $10\sigma$ ) was calculated to be 11 ppt. These results are consistent with previous ICP-TOFMS studies that show detection limits of approximately 1 ppt and at least four orders of magnitude LDR [36, 37, 39]. However, when the zoom-TOFMS instrument is operated in the CMA zoom mode at a 43.5 kHz repetition rate, the LDR of the instrument is expanded. The LDR for  $^{155}\text{Gd}^+$  detected with CMA-TOFMS at a 43.5 kHz repetition rate in Figure 5 is at least eight orders of magnitude. This expanded concentration range is due to a lower detection limit of 0.033 ppt (LOQ of 0.11 ppt) as the saturation point occurs for the nominally 10 ppm solution in both Supplementary Figure S-2 and Figure 5.

Detection limits for several elements in both zoom-TOFMS modes are compared in Table 2. On average, LODs for CMA-TOFMS were better than for CEA-TOFMS, even at the same repetition rate.

A detection limit is not reported in Table 2 for indium at 43.5 kHz in CMA zoom mode because the detection window for indium isotopes occurs at approximately 27  $\mu\text{s}$ . Acceleration pulses for a 43.5-kHz repetition rate are separated by 23  $\mu\text{s}$  and are 4.8  $\mu\text{s}$  in duration for indium. As a result, the indium detection and acceleration pulse windows overlap and noise from the acceleration pulse in the detection electronics corrupts the indium signal. Of course, noise from the acceleration pulse arises in the current detection setup regardless of operational mode. This noise limits the available range of frequencies for ion acceleration.

Two additional factors limit the repetition rate of the acceleration pulse in zoom-TOFMS, namely the fill-time of the acceleration region and the settling time of the acceleration pulse potential after a pulse has occurred. Fill time of the orthogonal-acceleration region was determined in a previous

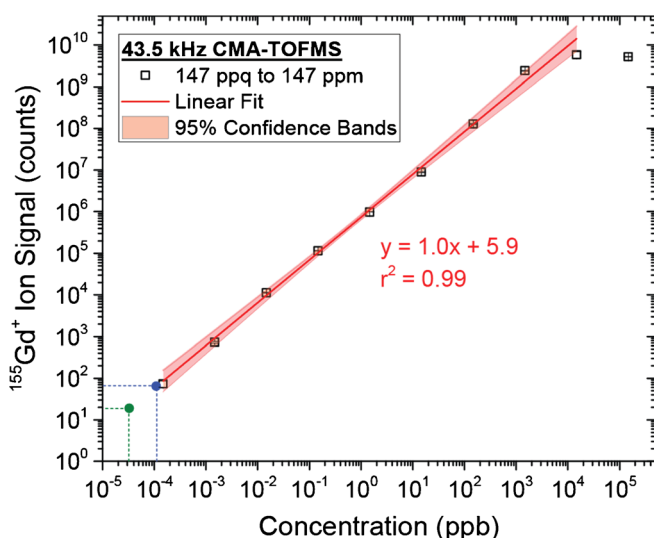


**Figure 5.** Linear dynamic range of the zoom-TOFMS system. Total ion signal for 60-s integration window for  $^{155}\text{Gd}^+$  (14.7% natural abundance) is shown for CMA-TOFMS at 43.5 kHz. The  $3\sigma$  limit-of-detection (LOD, green) and the  $10\sigma$  limit-of-quantitation (LOQ, blue) are indicated

zoom-TOFMS study to be 5  $\mu\text{s}$  for tin ions from a reduced-pressure, direct-current glow discharge [22]. Since ions produced in a hotter ICP source, are moving more quickly, and with a wider range of velocities into the acceleration region, the fill time here is less than 5  $\mu\text{s}$ . Unfortunately, the exact fill time could not be determined as it is not limiting—the settling time of the acceleration region is limiting in this system. For the current instrument geometry, the acceleration potential is applied to the repeller plate and across a series of electrodes (connected by resistors and capacitors in series) that total 10 cm in length. If the time between applied acceleration pulses is less than 21  $\mu\text{s}$ , the ion signal in successive detection windows is reduced and the ion focus distorted. Consequently, a maximum repetition rate of 43.5 kHz, which corresponds to 23  $\mu\text{s}$  pulse spacing, was used for CMA-TOFMS in this study.

The tens of parts-per-quadrillion (ppq) detection limits in Table 2 for Eu and Gd with 43.5 kHz CMA-TOFMS are considerably better than earlier results for ICP-TOFMS, which are typically in the high hundreds of ppq range [37, 39]. Of course, the background mass spectra from these interleaved CMA-TOFMS experiments have distinct, broad, low-intensity mass-spectral features because of defocused ions from other acceleration pulses. The detection limits reported are from a mass-spectral region where these features are absent. The lowest (best) detection limit reported in Table 2 is 0.024 ppt (24 ppq) for gadolinium with 60 s of integration time. Supplementary Figure S-3 shows that the detection limit of Gd for 43.5 kHz CMA-TOFMS improves from 0.18 ppt at 1 s integration time to 0.024 ppt at 60 s integration. The  $-0.55$  slope of the log-log plot in Supplementary Figure S-3 suggests that the detection limit is shot-noise limited. Also, at 1 s of integration time in CMA-TOFMS, the detection limit was found to be an order of magnitude better than the detection limit from CEA-TOFMS with 60 s of integration time.

To understand why CMA, zoom-mode detection limits are consistently lower than those obtained with conventional CEA-TOFMS (even at the same repetition rate), mass spectra that correspond to the results in Table 2 were analyzed for sensitivity and noise characteristics. On average, the sensitivities (cps/ppm) were an order of magnitude lower for CEA-TOFMS ( $2.0 \times 10^5$  cps/ppm) than for CMA-TOFMS at every repetition rate (10 kHz:  $2.3 \times 10^6$  cps/ppm, 20 kHz:  $5.2 \times 10^6$  cps/ppm, and 43.5 kHz:  $4.9 \times 10^6$  cps/ppm). Probable reasons for the sensitivity difference between CEA- and CMA-TOFMS are discussed above. The sensitivities corresponding to each of the reported detection limits in Table 2 are given in Supplementary Table S-2.

The additional gain in detection limits for higher repetition rates in CMA zoom mode is due to noise reduction. On average, the background mass-spectral noise [in cps per 10 ns of flight time (cps/10 ns)] dropped nearly an order of magnitude between the 20 kHz (6.3 cps/10 ns) and the 43.5 kHz (0.80 cps/10 ns) CMA-TOFMS detection limits. However, the noise was roughly the same between CEA- and CMA-TOFMS modes at 10 kHz (16 and 10 cps/10 ns, respectively). Specific background noise values for all reported detection limits in



Table 2 can be found in Supplementary Table S-3. The exact cause of noise reduction at higher repetition rates is unknown, but several possibilities exist. First, in all CMA-TOFMS experiments, energy filtering with the RPA and reflectron reduces the number of ions present in the flight tube at non-target masses, so background produced by scattered ions is reduced. In addition, a larger portion of the input ion beam is extracted at higher repetition rates, so fewer leakage ions enter the field-free region between acceleration pulses. These possibilities will be explored further in future studies.

## Conclusions

The ICP-zoom-TOFMS instrument is an intriguing alternative for the future of TOFMS. Ordinarily, enhanced resolution in TOFMS comes at the cost of lowered sensitivity and duty factor—this is not the case for zoom-TOFMS. In the zoom mode both mass resolution and sensitivity are improved for a narrow  $m/z$  range while background noise is reduced. Moreover, zoom-TOFMS is straightforward to incorporate into existing single-reflectron TOFMS instruments. In essence, all that is needed to retrofit an existing system for zoom-TOFMS operation is an acceleration region suited for the quick CMA pulses, a linear-field reflectron, and an RPA system to filter the ion beam. Zoom-TOFMS represents a relatively simple complementary function that is compatible with existing TOF instrumentation and is, therefore, an easily accessible technology.

## Acknowledgments

This work was funded in part by the U.S. Department of Energy through grant DE-FG02-98ER14890. The authors thank the Edward G. Blair, Mechanical Instrument Services and the Electronic Instrument Services facilities at Indiana University, for construction and subsequent modification of the ICP-zoom-TOFMS instrument. This work was performed in collaboration with Pacific Northwest National Laboratory, operated for the U.S. Department of Energy by Battelle Memorial Institute under contract DE-AC06-76RLO-1830op.

## References

1. Montaser, A. (ed.): *Inductively Coupled Plasma Mass Spectrometry*. Wiley, New York (1998)
2. Tanner, S.D., Holland, J.G. (ed.): *Plasma Source Mass Spectrometry: The New Millennium*. Royal Society of Chemistry, Cambridge, UK (2001)
3. Mueller, L., Traub, H., Jakubowski, N., Drescher, D., Baranov, V., Kneipp, J.: Trends in single-cell analysis by use of ICP-MS. *Anal. Bioanal. Chem.* **406**(27), 6963–6977 (2014)
4. Bandura, D.R., Baranov, V.I., Ornatsky, O.I., Antonov, A., Kinach, R., Lou, X., Pavlov, S., Vorobiev, S., Dick, J.E., Tanner, S.D.: Mass cytometry: technique for real time single cell multitarget immunoassay based on inductively coupled plasma time-of-flight mass spectrometry. *Anal. Chem.* **81**(16), 6813–6822 (2009)
5. Bendall, S.C., Simonds, E.F., Qiu, P., Amir, E.-A.D., Krutzik, P.O., Finck, R., Bruggner, R.V., Melamed, R., Trejo, A., Ornatsky, O.I., Balderas, R.S., Plevritis, S.K., Sachs, K., Pe'er, D., Tanner, S.D., Nolan, G.P.: Single-cell mass cytometry of differential immune and drug responses across a human hematopoietic continuum. *Science* **332**(6030), 687–696 (2011)
6. Beauchemin, D.: Inductively coupled plasma mass spectrometry. *Anal. Chem.* **80**(12), 4455–4486 (2008)
7. Arteav, V., Mitchell, J.C., Verentchikov, A., Yavor, M.: Multi-reflecting time-of-flight mass spectrometer and method of use. US7385187 B2 (2008)
8. Ioanoviciu, D.: The spiral main path electric deflector as a time-of-flight mass analyzer. *Int. J. Mass Spectrom.* **290**(2/3), 145–147 (2010)
9. Klitzke, C.F., Corilo, Y.E., Siek, K., Binkley, J., Patrick, J., Eberlin, M.N.: Petroleomics by ultrahigh-resolution time-of-flight mass spectrometry. *Energy Fuels* **26**(9), 5787–5794 (2012)
10. Satoh, T., Sato, T., Tamura, J.: Development of a high-performance MALDI-TOF mass spectrometer utilizing a spiral ion trajectory. *J. Am. Soc. Mass Spectrom.* **18**(7), 1318–1323 (2007)
11. Toyoda, M., Okumura, D., Ishihara, M., Katakuse, I.: Multi-turn time-of-flight mass spectrometers with electrostatic sectors. *J. Mass Spectrom.* **38**(11), 1125–1142 (2003)
12. Xian, F., Hendrickson, C.L., Marshall, A.G.: High resolution mass spectrometry. *Anal. Chem.* **84**(2), 708–719 (2012)
13. Leach, A.M., Hieftje, G.M.: Identification of alloys using single shot laser ablation inductively coupled plasma time-of-flight mass spectrometry. *J. Anal. At. Spectrom.* **17**, 852–857 (2002)
14. Leach, A.M., Hieftje, G.M.: Factors affecting the production of fast transient signals in single shot laser ablation inductively coupled plasma mass spectrometry. *Appl. Spectrosc.* **56**(1), 62–69 (2002)
15. Leach, A.M., Hieftje, G.M.: Standardless semiquantitative analysis of metals using single-shot laser ablation inductively coupled plasma time-of-flight mass spectrometry. *Anal. Chem.* **73**(13), 2959–2967 (2001)
16. Leach, A.M., Hieftje, G.M.: Methods for shot-to-shot normalization in laser ablation with an inductively coupled plasma time-of-flight mass spectrometer. *J. Anal. At. Spectrom.* **15**(9), 1121–1124 (2000)
17. Cotter, R.J.: Time-of-flight mass spectrometry. *Am. Chem. Soc.* **549**, 157–176 (1993)
18. Costa-Fernandez, J.M., Bings, N.H., Leach, A.M., Hieftje, G.M.: Rapid simultaneous multielemental speciation by capillary electrophoresis coupled to inductively coupled plasma time-of-flight mass spectrometry. *J. Anal. At. Spectrom.* **15**(9), 1063–1067 (2000)
19. Leach, A.M., Heisterkamp, M., Adams, F.C., Hieftje, G.M.: Gas chromatography inductively coupled plasma time-of-flight mass spectrometry for the speciation analysis of organometallic compounds. *J. Anal. At. Spectrom.* **15**, 151–155 (2000)
20. Mahoney, P.P., Ray, S.J., Li, G., Hieftje, G.M.: Preliminary investigations of electrothermal vaporization sample introduction for inductively coupled plasma-time-of-flight mass spectrometry. *Anal. Chem.* **71**, 1378–1383 (1999)
21. Guzowski Jr., J.P., Broekaert, J.A.C., Hieftje, G.M.: Electrothermal vaporization for sample introduction into a gas sampling glow discharge time-of-flight mass spectrometer. *Spectrochim. Acta B At. Spectrosc.* **55B**(8), 1295–1314 (2000)
22. Dennis, E., Gundlach-Graham, A., Ray, S., Enke, C., Barinaga, C., Koppelaar, D., Hieftje, G.: Zoom-TOFMS: addition of a constant-momentum-acceleration “zoom” mode to time-of-flight mass spectrometry. *Anal. Bioanal. Chem.* **406**(29), 7419–7430 (2014)
23. Cotter, R.J.: *Time-of-flight mass spectrometry: instrumentation and applications in biological research*, pp. 1–326. American Chemical Society, Washington. (1997)
24. Enke, C.G., Dobson, G.S.: Achievement of energy focus for distance-of-flight mass spectrometry with constant momentum acceleration and an ion mirror. *Anal. Chem.* **79**, 8650–8661 (2007)
25. Enke, C.G., Ray, S.J., Graham, A.W., Dennis, E.A., Hieftje, G.M., Carado, A.J., Barinaga, C.J., Koppelaar, D.W.: Distance-of-flight mass spectrometry: a new paradigm for mass separation and detection. *Annu. Rev. Anal. Chem.* **5**(1), 487–504 (2012)
26. Graham, A.W.G., Ray, S.J., Enke, C.G., Barinaga, C.J., Koppelaar, D.W., Hieftje, G.M.: First distance-of-flight instrument: opening a new paradigm in mass spectrometry. *J. Am. Soc. Mass Spectrom.* **22**, 110–117 (2011)
27. Graham, A.W.G., Ray, S.J., Enke, C.G., Felton, J.A., Carado, A.J., Barinaga, C.J., Koppelaar, D.W., Hieftje, G.M.: Resolution and mass range performance in distance-of-flight mass spectrometry with a multi-channel focal-plane camera detector. *Anal. Chem.* **83**(22), 8552–8559 (2011)
28. Gundlach-Graham, A., Dennis, E., Ray, S., Enke, C., Barinaga, C., Koppelaar, D., Hieftje, G.: Interleaved distance-of-flight mass

- spectrometry: a simple method to improve the instrument duty factor. *J. Am. Soc. Mass Spectrom.* **24**(11), 1736–1744 (2013)
29. Gundlach-Graham, A., Dennis, E.A., Ray, S.J., Enke, C.G., Barinaga, C.J., Koppenaal, D.W., Hieftje, G.M.: First inductively coupled plasma-distance-of-flight mass spectrometer: instrument performance with a microchannel plate/phosphor imaging detector. *J. Anal. At. Spectrom.* **28**(9), 1385–1395 (2013)
  30. Gundlach-Graham, A., Dennis, E.A., Ray, S.J., Enke, C.G., Barinaga, C.J., Koppenaal, D.W., Hieftje, G.M.: Laser-ablation sampling for inductively coupled plasma distance-of-flight mass spectrometry. *J. Anal. At. Spectrom.* **30**(1), 139–147 (2015)
  31. Gundlach-Graham, A.W., Dennis, E.A., Ray, S.J., Enke, C.G., Carado, A. J., Barinaga, C.J., Koppenaal, D.W., Hieftje, G.M.: Extension of the focusable mass range in distance-of-flight mass spectrometry with multiple detectors. *Rapid Commun. Mass Spectrom.* **26**(21), 2526–2534 (2012)
  32. Dennis, E., Ray, S., Gundlach-Graham, A., Enke, C., Barinaga, C., Koppenaal, D., Hieftje, G.: Constant-momentum acceleration time-of-flight mass spectrometry with energy focusing. *J. Am. Soc. Mass Spectrom.* **24**(12), 1853–1861 (2013)
  33. Dennis, E.A., Gundlach-Graham, A.W., Enke, C.G., Ray, S.J., Carado, A. J., Barinaga, C.J., Koppenaal, D.W., Hieftje, G.M.: How constant-momentum acceleration decouples energy and space focusing in distance-of-flight and time-of-flight mass spectrometries. *J. Am. Soc. Mass Spectrom.* **24**, 690–700 (2013)
  34. Gundlach-Graham, A.W.: Distance-of-flight mass spectrometry: theory, instrumentation, and practice. Indiana University (2013)
  35. Marcus, R.K., Broekaert, J.A.C.: *Glow Discharge Plasmas in Analytical Spectroscopy*. Wiley, Great Britain (2003)
  36. Borovinskaya, O., Hattendorf, B., Tanner, M., Gschwind, S., Gunther, D.: A prototype of a new inductively coupled plasma time-of-flight mass spectrometer providing temporally resolved, multi-element detection of short signals generated by single particles and droplets. *J. Anal. At. Spectrom.* **28**(2), 226–233 (2013)
  37. Sturgeon, R.E., Lam, J.W.H., Saint, A.: Analytical characteristics of a commercial ICP orthogonal acceleration time-of-flight mass spectrometer (ICP-TOFMS). *J. Anal. At. Spectrom.* **15**(6), 607–616 (2000)
  38. Guzowski Jr., J.P., Hieftje, G.M.: Characteristics of a rf-only hexapole ion-guide interface for plasma-source time-of-flight mass spectrometry. *J. Anal. At. Spectrom.* **16**(8), 781–792 (2001)
  39. Rogers, D.A., Ray, S.J., Hieftje, G.M.: An electrospray/inductively coupled plasma dual-source time-of-flight mass spectrometer for rapid metallomic and speciation analysis. Part 2. Atomic channel and dual-channel characterization. *Metallomics* **2**(4), 280–288 (2010)